Performance of Quasi-Degenerate Scaled Opposite Spin Perturbation Corrections to Single Excitation Configuration Interaction for Excited State Structures and Excitation Energies with Application to the Stokes Shift of 9-Methyl-9,10-dihydro-9-silaphenanthrene

Young Min Rhee,[†] David Casanova, and Martin Head-Gordon*

Department of Chemistry, University of California, Berkeley, California 94720, and Chemical Sciences Division, Lawrence Berkeley National Laboratory, Berkeley, California 94720

Received: April 21, 2009; Revised Manuscript Received: August 14, 2009

The quasi-degenerate scaled opposite spin perturbation correction to single excitation configuration interaction (SOS-CIS(D_0)) is a promising electronic structure method that can describe electronically excited states of sizable molecular systems. In this article, we report an assessment of the performance of SOS-CIS(D_0) for adiabatic electronic transition energies and excited state equilibrium geometries for various small molecules. These tests allow optimization of the empirical scaling parameter in SOS-CIS(D_0), and it is shown that one universal scaling parameter (chosen as 1.4) can satisfactorily reproduce the experimental results for all the tested molecules. The method is then applied to examine the large Stokes shift observed with a dihydrosilaphenanthrene derivative. The main features of the experimental absorption and emission spectra of this molecule are well reproduced by SOS-CIS(D_0).

1. Introduction

Developing electronic structure methods that can yield excited state energies reliably and efficiently has been a theme of research in quantum chemistry over many decades. It is also very important to have the analytical gradient of an excited state energy available. The gradient is a crucial tool in efficiently exploring and characterizing excited state potential energy surfaces and for enabling simulations of excited state dynamics. Presently, the most widely adopted approaches for excited state gradients are mean-field type methods such as time-dependent density functional theory (TDDFT)[1,2] and configuration interaction with single substitutions (CIS).[3,4] Even though there are many other more accurate excited state electronic structure methods with readily available analytic gradients, such as equation of motion coupled cluster (EOM-CC) approaches,[5,6] the high associated computational costs have prohibited their application to sizable molecules.

Therefore there are ongoing efforts to develop alternative excited state methods which offer accuracy that is greater than mean-field type methods with computational cost that is significantly less than full EOM-CC models. For instance, the "second order coupled cluster" (CC2) approach is an approximation to full singles and doubles coupled cluster (CCSD) theory with reasonable accuracy and computational costs that scale as $O(M^5)$ with molecular size for both energy and gradient,[7,8] in contrast to $O(M^6)$ for CCSD. Another developmental effort comes from a perturbative treatment of the electron correlation, which led to both nondegenerate doubles (CIS(D)[9]) and quasi-degenerate doubles corrections (CIS(D_0) and CIS(D_1)[10]) to CIS. These methods also exhibit $O(M^5)$ scaling.

Recently, we established that comparable or even improved accuracy could by obtained with only $O(M^4)$ cost by performing the correlation corrections only for electrons with opposite spins, and semiempirically scaling the resulting correction. Scaled opposite spin (SOS) approaches were first developed as lower scaling modifications to second order Møller−Plesset (MP2) theory for the ground state energy[11,12] and gradient,[13] as a valuable special case of the spin component scaling concept pioneered by Grimme and co-workers.[14−16] Reduced scaling requires the combination of resolution of the identity (RI) approximation for the integrals with the Laplace transform technique for inverting denominators proposed by Almlöf and co-workers.[17,18] In fact, this combination is also being adopted in the development of various other fast electron correlation methods.[19,20] We have also formulated and tested $O(M^4)$ nondegenerate[21] and quasi-degenerate[22] scaled opposite spin doubles corrections to CIS. The latter, termed SOS-CIS(D_0), is particularly appropriate for exploring excited state potential surfaces where crossings may be encountered, and so, very recently, we have also formulated and implemented its analytic gradient, again, in a fast fourth-order scaling manner.[23]

The first purpose of this article is to assess the performance of SOS-CIS(D_0), for the calculation of adiabatic electronic transition energies and the equilibrium excited state geometries against experimental data for various small molecules. SOS-CIS(D_0) has one empirical scaling parameter, which is the factor by which excited state opposite spin correlations should be enhanced to account for the neglect of explicit same-spin correlations. In our original formulation,[22] we simply transferred its numerical value from the related SOS-CIS(D) theory, partly due to the lack of an analytic gradient with which to broadly test the performance of the method. We are now in a position to revisit this question more carefully, and we will show that one universal scaling parameter can be found that satisfactorily reproduces the experimental results for all the tested molecules. SOS-CIS(D_0) is then applied to explain the peculiarly large Stokes shift observed experimentally[24] in the 9-methyl-9,10-dihydro-9-silaphenanthrene molecule. Through the use of the gradient of the optimized SOS-CIS(D_0), we show that the experimental absorption and emission features of this molecule

* Corresponding author, mhg@cchem.berkeley.edu.
[†] Present address: Department of Chemistry, Pohang University of Science and Technology, Pohang 790-784, Korea.

10.1021/jp903659u CCC: $40.75
Published on Web 09/08/2009

are well explained. We conclude with a short discussion of the prospects for further methodological improvements in the future.

2. Theory

Complete details of the SOS-CIS(D_0) theory and the derivation of its analytical gradient can be found elsewhere.[22,23] For completeness, we will briefly overview the working expressions of these previous developments. The excitation energy is found as an eigenvalue ω of the symmetrized SOS-CIS(D_0) response matrix

$$[\mathbf{A}_{SS}^{(0)} + c_T\mathbf{A}_{SS}^{(2)} + c_U\mathbf{A}_{SD}^{(1)}(\mathbf{D}_{DD}^{(0)})^{-1}\mathbf{A}_{DS}^{(1)}]\mathbf{b} = \omega\mathbf{b} \quad (1)$$

Here, c_T and c_U represent the opposite spin component scaling parameters of the indirect and direct perturbation correction terms, respectively. Of course, the corresponding excitation amplitude vector $\mathbf{b}$ for the state of interest is simultaneously computed with the excitation energy. Because $\mathbf{b}$ is an eigenvector of the response matrix, the first derivative of ω does not require the evaluation of any derivative of $\mathbf{b}$. Thus, the analytical gradient is obtained as

$$\omega^{(x)} = \mathbf{b}[\mathbf{A}_{SS}^{(0)}]^{(x)}\mathbf{b} + c_T\mathbf{b}[\mathbf{A}_{SS}^{(2)}]^{(x)}\mathbf{b} + c_U\mathbf{b}[\mathbf{A}_{SD}^{(1)}(\mathbf{D}_{DD}^{(0)})^{-1}\mathbf{A}_{DS}^{(1)}]^{(x)}\mathbf{b} \quad (2)$$

As in other perturbation schemes, the second-order correction terms of the response matrix involve energy denominators. The quartic-scaling SOS-CIS(D_0) utilizes the Laplace transform for the energy denominator[1−4]

$$\frac{1}{\Delta_{ij}^{ab}} = \sum_t \rho_t \exp(-\Delta_{ij}^{ab}t) \quad (3)$$

together with the resolution-of-the-identity (RI) approximation[25−32]

$$(pq|rs)_{RI} = \sum_{PQ}(pq|P)(P|Q)^{-1}(Q|rs) = \sum_R B_{pq}^R B_{rs}^R \quad (4)$$

for electron repulsion integrals (ERIs). Here, ρ_t denotes the weight at any given quadrature point t, $\mathbf{\Delta}$ represents the diagonal energy difference tensor $\Delta_{ij}^{ab} = \varepsilon_a + \varepsilon_b - \varepsilon_i - \varepsilon_j$, and $\mathbf{B}$ is an ERI-related matrix consisting of the contraction of three center integrals with the inverse square root of the two-center integrals: $B_{pq}^R = \sum_p (pq|P)(P|R)^{-1/2}$.

Because the excitation energy is not stationary with respect to the mixing of molecular orbitals, its analytical gradient should include the orbital response elements in its expression. As any arbitrary occupied−occupied and virtual−virtual orbital mixing does not change the excitation energy, symmetric orbital response[33,34] is often enforced in gradient theory for mathematical convenience

$$U_{ij}^x = -\frac{1}{2}S_{ij}^x \quad (5a)$$

$$U_{ab}^x = -\frac{1}{2}S_{ab}^x \quad (5b)$$

with $\mathbf{S}^x$ matrices denoting the derivatives of the overlap integrals. One drawback of using this scheme is the fact that the energy difference tensor $\mathbf{\Delta}$ is not diagonal any more after the geometric distortion "x". This complicates the formulation of the first derivative of $e^{-\mathbf{\Delta}t}$ because a tensor $\mathbf{\Delta}$ and its derivative $\mathbf{\Delta}^{(x)}$ do not commute unless both are diagonal. On the basis of Brillouin's theorem,[35] however, $\mathbf{\Delta}^{(x)}$can always be represented as block-diagonal. Using this property, one can show that the following equation is satisfied

$$[e^{-\mathbf{\Delta}t}]_{ijab;i'j'a'b'}^{(x)} = -t\delta_{ii'}\delta_{jj'}\varepsilon_{aa'}^{(x)}\delta_{bb'}e^{-\Delta_{ij}^{ab}t}h(\Delta_a^{a'}t) - t\delta_{ii'}\delta_{jj'}\delta_{aa'}\varepsilon_{bb'}^{(x)}e^{-\Delta_{ij}^{ab}t}h(\Delta_b^{b'}t) + t\varepsilon_{ii'}^{(x)}\delta_{jj'}\delta_{aa'}\delta_{bb'}e^{-\Delta_{ij}^{ab}t}h(\Delta_i^{i'}t) + t\delta_{ii'}\varepsilon_{jj'}^{(x)}\delta_{aa'}\delta_{bb'}e^{-\Delta_{ij}^{ab}t}h(\Delta_j^{j'}t) \quad (6)$$

with $h(x) = (1 - e^{-x})/x$ and $\Delta_p^q = \varepsilon_q - \varepsilon_p$.[23] This equation greatly simplifies the derivation of the analytical gradient of SOS-CIS(D_0), whose working expression can be expressed in a compact form

$$[\omega]^{(x)} = 2\Theta_{ai}^P(ai|P)^x - \gamma_{RS}(R|S)^x + W_{ab}S_{ab}^x + 2W_{ai}S_{ai}^x + W_{ij}S_{ij}^x + P_{ab}\varepsilon_{ab}^{(x)} + P_{ij}\varepsilon_{ij}^{(x)} + 2L_{ai}U_{ai}^x + 2M_{aj}^P b_j^b(ab|P)^x - 2M_{bj}^P b_i^b(ij|P)^x \quad (7)$$

Presenting the complete expressions of the various one-particle and two-particle density matrices and the Lagrangian will be beyond the scope of this article, and curious readers should refer to ref 23 for the details. The purpose of presenting this rather symbolic equation is to show the apparent similarity between gradient expressions from SOS-CIS(D_0) and other second-order perturbative schemes with the RI approximation.[30]

After replacing the orbital response term through the use of the Handy−Schaefer device,[36] the final working gradient expression can be written as

$$E_{SOS\text{-}CIS(D_0)}^{(x)} = P_{\mu\nu}^{tot}H_{\mu\nu}^x + W_{\mu\nu}^{tot}S_{\mu\nu}^x + 2\Gamma_{\mu\nu}^{tot;P}(\mu\nu|P)^x - \gamma_{RS}^{tot}(R|S)^x + \Gamma_{\mu\nu\lambda\sigma}^{tot}(\mu\nu|\lambda\sigma)^x \quad (8)$$

Here, we have used "tot" to denote that the density matrices should include contributions from all relevant energy terms (HF, SOS-MP2, and ω).[23]

3. Optimization of the Parameter c_U

The scaling parameter c_U inevitably influences the character of any excited state potential energy surface obtained with SOS-CIS(D_0). Thus, a proper choice of its numerical value will be crucial for its reliability. Too small a value (for instance 1 or smaller) will clearly underestimate electron correlation effects since same-spin correlations are not explicitly considered. Too large a value (for instance 2 or larger) will likewise lead to exaggerated correlation effects. Because changes in the excited state potential energy surface due to changes in the parameter, c_U, change both the excited state equilibrium geometries and adiabatic electronic excitation energies, these two aspects should both be considered in searching for the optimal value of this empirical parameter. Of course, it will be desirable to have one

TABLE 1: Adiabatic Transition Energies (T_e) of the Training Set with aug-cc-pVDZ Basis[a]

		c_U							
molecule	state	1.30	1.35	1.40	1.45	1.51	CC2	CIS	exp[b]
Li_2[c]	$1^1\Sigma_u^+$	1.97	1.94	1.91	1.88	1.84	1.90	2.10	1.74
BH	$1^1\Pi$	3.02	2.98	2.94	2.90	2.85	2.87	2.84	2.87
BF	$1^1\Pi$	6.60	6.55	6.49	6.44	6.37	6.38	6.51	6.34
	$1^3\Pi$	3.43	3.41	3.39	3.36	3.33	3.25	2.63	3.61
	$1^3\Sigma^+$	7.95	7.92	7.89	7.86	7.83	7.56	7.39	7.57
N_2	$1^3\Pi_g$	7.82	7.73	7.63	7.54	7.43	7.12	7.56	7.39
	$1^1\Sigma_u^-$	8.96	8.89	8.82	8.75	8.67	8.56	7.31	8.45
	$1^1\Pi_g$	9.09	8.97	8.84	8.72	8.58	8.29	9.43	8.59
	$1^1\Delta_u$	9.45	9.37	9.29	9.22	9.12	9.22	7.94	8.94
CO	$1^1\Pi$	8.50	8.39	8.29	8.18	8.05	7.91	8.73	8.07
	$1^3\Pi$	6.37	6.31	6.26	6.20	6.13	5.95	5.72	6.04
Mg_2[c]	$1^1\Sigma_u^+$	3.46	3.43	3.40	3.37	3.33	3.25	3.33	3.23
SiO	$1^1\Pi$	4.96	4.82	4.68	4.54	4.36	4.65	5.96	5.31
	$1^3\Delta$	3.62	3.44	3.26	3.07	2.84	3.47	4.70	4.52
H_2O	$2\ ^1B_1$	11.11	11.00	10.89	10.78	10.64	8.91	12.07	10.00
SO_2	$1\ ^3B_1$	2.91	2.76	2.60	2.43	2.25	2.56	2.46	3.19
SiF_2	$1\ ^1B_1$	5.65	5.56	5.47	5.38	5.27	5.46	5.92	5.34
CCl_2	$1\ ^1B_1$	2.37	2.28	2.19	2.10	1.99	2.24	2.26	2.14
CS_2	$1\ ^3A_2$	3.21	3.10	2.99	2.88	2.74	3.17	3.39	3.25
HCN	$1\ ^1A''$	6.90	6.83	6.75	6.68	6.59	6.55	5.55	6.48
HCP	$1\ ^1A''$	4.62	4.56	4.50	4.44	4.36	4.43	3.51	4.31
C_3	$1\ ^1\Pi_u$	3.90	3.76	3.64	3.51	3.37	3.09	4.39	3.06
C_2H_2	$1\ ^1A_u$	5.28	5.21	5.13	5.05	4.96	5.09	4.39	5.23
CH_2O	$1\ ^1A''$	3.60	3.44	3.27	3.10	2.86	3.44	4.39	3.49
	$1\ ^3A''$	3.17	3.04	2.90	2.77	2.60	2.93	3.49	3.12
CH_2S	$1\ ^1A_2$	2.17	2.06	1.94	1.82	1.68	2.13	2.61	2.03
	$1\ ^3A''$	1.90	1.80	1.71	1.61	1.49	1.74	1.92	1.80
trans-$(CHO)_2$	$1\ ^1A_u$	3.08	2.93	2.77	2.62	2.43	2.67	3.55	2.72
HC_2CHO	$1\ ^1A''$	3.36	3.16	2.97	2.76	2.52	3.08	4.42	3.24
MSE[d]		0.22	0.12	0.03	−0.07	−0.21	−0.14	0.15	
MAE[e]		0.34	0.30	0.30	0.31	0.36	0.22	0.63	
RMSE[f]		0.42	0.39	0.40	0.43	0.53	0.36	0.78	
MAXE[g]		1.11	1.08	1.26	1.45	1.68	1.09	2.07	

[a] The ground and excited state geometries were optimized using SOS-MP2 and SOS-CIS(D_0) theories, respectively. The parameter c_T was fixed at 1.30 as suggested in SOS-MP2 theory (ref 11). In electronvolts. [b] Experimental references are summarized in ref 7. [c] Basis set defined in ref 7. [d] Mean signed error. [e] Mean absolute error. [f] Root-mean-square error. [g] Maximum absolute error.

universal parameter that can be applied to any arbitrary chemical systems, and a primary purpose of our test calculations will be to assess the extent to which this is possible in practice.

In our previous work where the SOS-CIS(D_0) method was first proposed and implemented, we have shown that this scaling scheme with one fixed empirical parameter can be reliable and robust at least for a wide range of organic molecules.[22] In that work, we employed CIS-optimized excited state geometries and HF-optimized ground state geometries in order to perform computational tests of SOS-CIS(D_0) adiabatic excitation energies. This choice was due to the lack of the SOS-CIS(D_0) analytical gradient at that initial stage of development. However, it is well-known that true mean-field methods such as HF and CIS tend to overestimate the "tightness" of molecules: shorter bond lengths and higher vibrational frequencies are obtained compared to more reliable electron correlated theories and experiment, essentially because electrons approach each other slightly too closely as a consequence of neglect of correlations. Thus, assessing the scaling parameter based on HF/CIS geometries may have introduced some systematic error in the performance of SOS-CIS(D_0). As we now have analytical gradient theory of SOS-CIS(D_0) at hand, we are in a perfect position to revisit the optimization of this parameter.

Even though it would be desirable to adopt the same set of organic molecules as in our previous work (in terms of the size, ranging from acetone to pyrene),[22] the total computation time will be annoyingly long for excited state geometry optimizations for large organic molecules especially with large basis sets. More importantly, experimental excited state geometries are not known for these large molecules—only the excitation energies are available. For these practical reasons, we will only use a set of small molecules for calibration calculations. In fact, Furche and Ahlrichs have accumulated an excellent test set for assessing the performance of TDDFT for excited state properties,[2] which Köhn and Hättig later expanded for demonstrating the performance of CC2 excited state gradient theory.[7] As CC2 has a direct relevance to our new theory as explained in the Introduction, we will adopt Köhn and Hättig's test set for the parameter optimization. A developmental version of Q-Chem 3.2[37] was used in all computations presented in this work.

Table 1, 2, and 3 list the adiabatic energies for selected transitions of these test molecules with a range of different scaling parameters. Three different correlation consistent basis sets were used in generating these tables. As noted in ref 7, simply examining overall statistics may not be entirely adequate for evaluating the results, as its result may depend on the choice of the test molecules. In addition, there are other uncertainties in comparing the results with the experimental numbers. For example, experimental evaluation of the adiabatic transition energies (T_e) of diatomic molecules involves corrections for the zero point energies, which are not directly measured but estimated based on some model Hamiltonian.[7] Additionally, the

TABLE 2: Adiabatic Transition Energies of the Training Set with aug-cc-pVTZ Basis[a]

		c_U							
molecule	state	1.30	1.35	1.40	1.45	1.51	CC2	CIS	exp[b]
Li_2[c]	$1^1\Sigma_u^+$	2.01	1.98	1.94	1.91	1.86	1.91	2.10	1.74
BH	$1^1\Pi$	2.98	2.93	2.88	2.83	2.76	2.83	2.85	2.87
BF	$1^1\Pi$	6.61	6.55	6.48	6.42	6.34	6.38	6.56	6.34
	$1^3\Pi$	3.62	3.59	3.56	3.53	3.49	3.39	2.73	3.61
	$1^3\Sigma^+$	7.95	7.92	7.89	7.86	7.83	7.54	7.27	7.57
N_2	$1^3\Pi_g$	8.05	7.94	7.83	7.72	7.59	7.25	7.69	7.39
	$1^1\Sigma_u^-$	9.10	9.02	8.93	8.84	8.73	8.65	7.49	8.45
	$1^1\Pi_g$	9.23	9.09	8.95	8.81	8.64	8.35	9.58	8.59
	$1^1\Delta_u$	9.60	9.50	9.41	9.31	9.20	9.31	8.11	8.94
CO	$1^1\Pi$	8.59	8.47	8.35	8.23	8.09	7.93	8.80	8.07
	$1^3\Pi$	6.53	6.46	6.39	6.32	6.24	6.03	5.76	6.04
Mg_2[c]	$1^1\Sigma_u^+$	3.33	3.30	3.26	3.22	3.18	3.21	3.32	3.23
SiO	$1^1\Pi$	5.23	5.08	4.93	4.77	4.59	4.74	6.12	5.31
	$1^3\Delta$	4.15	3.97	3.79	3.59	3.36	3.71	4.93	4.52
H_2O	$2\ ^1B_1$	10.98	10.86	10.75	10.64	10.50	9.11	11.74	10.00
SO_2	$1\ ^3B_1$	3.31	3.15	3.00	2.84	2.65	2.86	3.05	3.19
SiF_2	$1\ ^1B_1$	5.73	5.64	5.55	5.45	5.34	5.49	5.92	5.34
CCl_2	$1\ ^1B_1$	2.23	2.12	2.01	1.91	1.78	2.13	2.18	2.14
CS_2	$1\ ^3A_2$	3.38	3.26	3.13	3.00	2.85	3.27	3.30	3.25
HCN	$1\ ^1A''$	7.03	6.94	6.86	6.77	6.66	6.68	5.65	6.48
HCP	$1\ ^1A''$	4.67	4.60	4.52	4.44	4.35	4.45	3.61	4.31
C_3	$1\ ^1\Pi_u$	3.90	3.76	3.62	3.48	3.32	3.09	4.43	3.06
C_2H_2	$1\ ^1A_u$	5.53	5.44	5.36	5.27	5.17	5.29	4.57	5.23
CH_2O	$1\ ^1A''$	3.75	3.58	3.40	3.22	3.00	3.49	4.44	3.49
	$1\ ^3A''$	3.34	3.19	3.04	2.90	2.72	3.01	3.69	3.12
CH_2S	$1\ ^1A_2$	2.22	2.09	1.96	1.84	1.67	2.13	2.61	2.03
	$1\ ^3A''$	1.96	1.85	1.75	1.64	1.51	1.77	1.86	1.80
trans-$(CHO)_2$	$1\ ^1A_u$	3.15	2.98	2.81	2.64	2.44	2.69	2.72	2.72
HC_2CHO	$1\ ^1A''$	3.50	3.30	3.09	2.87	2.61	3.14	4.49	3.24
MSE		0.33	0.22	0.12	0.01	−0.12	−0.08	0.22	
MAE		0.36	0.28	0.26	0.26	0.29	0.18	0.61	
RMSE		0.43	0.37	0.33	0.33	0.38	0.29	0.74	
MAXE		0.98	0.86	0.75	0.93	1.16	0.89	1.74	

[a] See Table 1 for other details. In electronvolts. [b] Experimental references are summarized in ref 7. [c] Basis set defined in ref 7.

basis set requirements for Rydberg states differ strongly from that for valence states. However, with these caveats, the overall error level from using a specific value of c_U can still be estimated from some representative metrics such as mean signed errors (MSEs) and mean absolute errors (MAEs).

When Tables 1−3 are inspected, the first general trend that is evident is that for a given basis set, the excitation energies are largest with the smallest value of c_U and then steadily decrease as this parameter is increased. This trend follows directly from the defining equation, eq 1, since c_U scales an excited state energy term that is negative-definite, corresponding to the extent of correlation of electron pairs that involve at least one electron active in the transition. The second observation one can make is that the optimal scaling parameter seems to lie within the 1.35−1.45 range, with slightly larger values preferred with larger basis sets. There is not a sharp optimal value, but nevertheless, this range of values is somewhat smaller than the optimal scaling parameter, $c_U = 1.51$, previously reported for the sister theory, SOS-CIS(D).[21] As the SOS-CIS(D) optimization of c_U was based on noncorrelated CIS geometries, and as SOS-CIS(D) has a different scheme of treating the excitation response matrix, this small discrepancy is not actually a surprising result. The third observation that can be made is that the mean absolute error (i.e., for the best value of the scaling parameter, c_U) decreases quite noticeably as the basis set size is increased. This is an encouraging result, because lower errors for larger basis sets suggest that the method has sound physical content. It is also accompanied by a significantly smaller maximum absolute error in the largest basis set.

Instead of trying to immediately select the best value of the scaling parameter from the data in these tables, let us next consider the behavior of results for optimized excited state geometries. Tables 4, 5, and 6 show the equilibrium excited state geometrical parameters for the same molecules with the same basis. While there is much data in these tables, most of it can be summarized as several main observations. The first observation is that SOS-CIS(D_0) tends to slightly overestimate most bond lengths for the test molecules. As already discussed earlier, CIS tends to significantly underestimate excited state equilibrium bond lengths, and therefore our second-order perturbation correction slightly overcorrects. However, the degree of overestimation is usually acceptable (on average, the errors are around a few picometers) regardless of c_U and smaller than those normally associated with CIS. The second main observation is that while the quality of results depends fairly weakly on the value of c_U, the results become more reliable with smaller scaling parameters. Smaller values of c_U reduce the effect of electron correlation in the excited state and therefore reduce the overcorrection. A similar trend can also be found with the bond angles of the test molecules. This differs somewhat from the conclusion for optimal c_U values seen for adiabatic excitation energies. The third point is that the quality of results improves significantly upon improvement of the basis from augmented double-ζ to triple-ζ to quadruple-ζ.

TABLE 3: Adiabatic Transition Energies of the Training Set with aug-cc-pVQZ Basis[a]

		c_U							
molecule	state	1.30	1.35	1.40	1.45	1.51	CC2	CIS	exp[b]
BH	$1^1\Pi$	2.97	2.92	2.86	2.80	2.74	2.82	2.85	2.87
BF	$1^1\Pi$	6.59	6.52	6.45	6.38	6.30	6.37	6.56	6.34
	$1^3\Pi$	3.65	3.62	3.59	3.56	3.52	3.42	2.73	3.61
	$1^3\Sigma^+$	7.99	7.96	7.93	7.90	7.87	7.55	7.24	7.57
N_2	$1^3\Pi_g$	8.07	7.96	7.84	7.73	7.59	7.29	7.71	7.39
	$1^1\Sigma_u^-$	9.09	8.99	8.90	8.80	8.69	8.69	7.52	8.45
	$1^1\Pi_g$	9.22	9.07	8.92	8.78	8.60	8.38	9.60	8.59
	$1^1\Delta_u$	9.58	9.48	9.37	9.27	9.15	9.35	8.13	8.94
CO	$1^1\Pi$	8.59	8.46	8.34	8.21	8.06	7.96	8.82	8.07
	$1^3\Pi$	6.55	6.48	6.41	6.34	6.25	6.07	5.78	6.04
SiO	$1^1\Pi$	5.35	5.19	5.04	4.88	4.69	4.77	6.15	5.31
	$1^3\Delta$	4.32	4.14	3.95	3.76	3.52	3.78	4.37	4.52
H_2O	$2\ ^1B_1$	10.90	10.78	10.67	10.56	10.42	9.20	11.56	10.00
SO_2	$1\ ^3B_1$	3.44	3.28	3.13	2.97	2.77	2.92	3.08	3.19
SiF_2	$1\ ^1B_1$	5.74	5.65	5.56	5.46	5.34	5.49	5.92	5.34
CCl_2	$1\ ^1B_1$	2.20	2.09	1.98	1.87	1.73	2.11	2.16	2.14
CS_2	$1\ ^3A_2$	3.39	3.26	3.13	2.99	2.83	3.29	3.40	3.25
HCN	$1\ ^1A''$	7.07	6.97	6.88	6.79	6.67	6.72	5.72	6.48
HCP	$1\ ^1A''$	4.69	4.61	4.53	4.44	4.34	4.48	3.64	4.31
C_3	$1\ ^1\Pi_u$	3.89	3.75	3.61	3.47	3.30	3.09	4.43	3.06
C_2H_2	$1\ ^1A_u$	5.56	5.47	5.38	5.29	5.17	5.33	4.58	5.23
CH_2O	$1\ ^1A''$	3.78	3.61	3.43	3.24	3.02	3.52	4.45	3.49
	$1\ ^3A''$	3.38	3.23	3.08	2.93	2.75	3.05	3.54	3.12
CH_2S	$1\ ^1A_2$	2.25	2.11	1.98	1.84	1.67	2.15	2.51	2.03
	$1\ ^3A''$	2.00	1.89	1.77	1.66	1.52	1.79	1.89	1.80
trans-$(CHO)_2$	$1\ ^1A_u$	3.17	3.00	2.82	2.64	2.43	2.70	3.59	2.72
HC_2CHO	$1\ ^1A''$	3.54	3.33	3.12	2.90	2.63	3.17	4.50	3.24
MSE		0.37	0.25	0.13	0.01	−0.13	−0.06	0.24	
MAE		0.38	0.29	0.24	0.25	0.28	0.18	0.65	
RMSE		0.45	0.36	0.31	0.30	0.36	0.27	0.81	
MAXE		0.90	0.78	0.67	0.76	1.00	0.80	1.92	

[a] See Table 1 for other details. In electronvolts. [b] Experimental references are summarized in ref 7.

As noted above, there is some conflict between the conclusions based on excited state structures and the conclusions based on adiabatic excitation energies as to the optimal value of c_U that should be employed for general use. This conflict is not serious because the quality of either set of results does not depend strongly on small changes in c_U. On the basis of the detailed observations and discussions above, we propose to use $c_U = 1.40$ as the optimal parameter. Even though a larger value may lead to slightly more accurate adiabatic excitation energies with a large basis set such as aug-cc-pVQZ (Table 3), using such a large basis set will not be practical for many realistic molecules. In addition, excited state equilibrium geometries are usually slightly better at $c_U = 1.40$ compared to the case with a larger scaling parameter. Even though the resulting excitation energy will have a small systematic error with a large enough basis set (~0.1 eV overestimation in Table 3), this is insignificant compared to the intrinsic uncertainty of any second-order perturbative treatments for the excitation energy calculations.

It will also be informative to observe how this newly optimized scaling parameter affects the accuracy of SOS-CIS(D_0) in predicting electronic transitions in relatively large organic molecules. For this observation, we again have adopted the test set compiled by Grimme and co-workers.[15] This comparison will be especially important because our training set for the parameter optimization in this work was only limited to small molecules, and we should confirm that the method is transferable to larger systems. In this check, we adopted two sets of basis functions, a large and likely reliable basis (aug-cc-pVTZ) and a significantly smaller and potentially less reliable basis (6-31+G(d)). Table 7 presents the results obtained with the two basis sets. When the error levels with the aug-cc-pVTZ basis set are compared with the matching numbers in Table 2 with $c_U = 1.40$, one can easily see that the results are quite comparable. This is an encouraging result, as it directly shows good transferability of the parameter. The error levels from calculations with the 6-31+G(d) basis set are somewhat inferior to the aug-cc-pVTZ results. However, the difference is only marginal (also see Figure 1) and the 6-31+G(d) results are at least comparable to the small molecule results presented in Table 1 with aug-cc-pVDZ. Therefore, we can infer that at least for the valence transitions described in this table, relatively small basis sets can be used without noticeably sacrificing the accuracy. It should also be mentioned that selecting a basis set that can adequately describe the target excited states is crucial to obtaining good results: for example, when a similarly sized basis set, 6-31G(d,p), without diffuse functions, was adopted, there were clear deviations especially for states with high excitation energies.

Finally we conclude with some discussion about the overall performance of SOS-CIS(D_0) relative to other excited state electronic structure methods. Relative to the uncorrelated CIS method, there is significant improvement in excitation energies (as also established previously[22]) and useful improvement in the quality of excited state equilibrium geometries. Relative to the CC2 method, which has computational costs that scale one power of system size higher, the overall quality of our results is generally comparable, though in detail slightly inferior. Given the significant difference in computational cost, this is encouraging from the point of view of further reducing cost. However, it must be noted that generally the performance of both of these

TABLE 4: Geometrical Parameters Optimized with aug-cc-pVDZ Basis[a,b]

			c_U							
molecule	state	parameter	1.30	1.35	1.40	1.45	1.51	CC2	CIS	exp[c]
Li_2[d]	$1^1\Sigma_u^+$	r_e	3.167	3.171	3.178	3.181	3.184	3.131	3.096	3.107
BH	$1^1\Pi$	r_e	1.226	1.226	1.227	1.227	1.227	1.227	1.214	1.219
BF	$1^1\Pi$	r_e	1.358	1.359	1.361	1.363	1.365	1.365	1.317	1.304
	$1^3\Pi$	r_e	1.359	1.359	1.359	1.359	1.359	1.365	1.330	1.308
	$1^3\Sigma^+$	r_e	1.241	1.242	1.242	1.242	1.242	1.257	1.224	1.215
N_2	$1^3\Pi_g$	r_e	1.238	1.238	1.239	1.240	1.241	1.268	1.185	1.213
	$1^1\Sigma_u^-$	r_e	1.286	1.286	1.286	1.286	1.291	1.322	1.286	1.276
	$1^1\Pi_g$	r_e	1.253	1.253	1.254	1.255	1.256	1.284	1.199	1.220
	$1^1\Delta_u$	r_e	1.284	1.284	1.285	1.286	1.286	1.310	1.237	1.268
CO	$1^1\Pi$	r_e	1.290	1.293	1.296	1.299	1.303	1.315	1.221	1.235
	$1^3\Pi$	r_e	1.226	1.227	1.228	1.229	1.230	1.248	1.184	1.206
Mg_2[d]	$1^1\Sigma_u^+$	r_e	3.135	3.134	3.132	3.131	3.130	3.147	3.242	3.082
SiO	$1^1\Pi$	r_e	1.794	1.799	1.804	1.810	1.815	1.828	1.630	1.620
	$1^3\Delta$	r_e	1.998	2.014	2.028	2.041	2.054	1.886	1.683	1.715
H_2O	$2\ ^1B_1$	d(OH)	1.012	1.013	1.014	1.016	1.018	1.043	0.969	1.069
		∠(HOH)	104.8	104.7	104.7	104.6	104.5	102.6	109.0	101.6
SO_2	$1\ ^3B_1$	d(SO)	1.568	1.572	1.576	1.580	1.586	1.629	1.552	1.494
		∠(OSO)	125.5	125.2	124.9	124.5	124.1	130.2	104.0	126.1
SiF_2	$1\ ^1B_1$	d(SiF)	1.683	1.686	1.688	1.691	1.695	1.684	1.624	1.601
		∠(FSiF)	116.6	116.8	117.0	117.3	117.4	116.8	111.5	115.9
CCl_2	$1\ ^1B_1$	d(CCl)	1.692	1.693	1.694	1.695	1.696	1.674	1.667	1.652
		∠(ClCCl)	131.2	131.2	131.1	131.0	131.0	131.1	131.8	131.4
CS_2	$1\ ^3A_2$	d(CS)	1.666	1.668	1.669	1.670	1.671	1.671	1.614	1.64
		∠(SCS)	133.3	133.2	133.0	132.9	132.9	134.4	140.4	135.8
HCN	$1^1A''$	d(CH)	1.132	1.133	1.133	1.134	1.135	1.132	1.104	1.140
		d(CN)	1.308	1.308	1.308	1.308	1.308	1.339	1.293	1.297
		∠(HCN)	123.5	123.5	123.6	123.7	123.8	121.5	119.7	125.0
HCP	$1^1A''$	d(CP)	1.719	1.718	1.718	1.717	1.717	1.742	1.701	1.69
		∠(HCP)	127.2	127.4	127.5	127.9	127.9	125.6	128.1	128.0
C_3	$1^1\Pi_u$	d(CC)	1.325	1.325	1.325	1.326	1.326	1.346	1.296	1.305
C_2H_2	1^1A_u	d(CC)	1.391	1.392	1.392	1.393	1.394	1.401	1.363	1.375
		d(CH)	1.108	1.108	1.108	1.108	1.108	1.107	1.089	1.105
		∠(HCC)	120.8	120.7	120.6	120.5	120.4	121.0	124.0	121.4
CH_2O	$1^1A''$	d(CH)	1.101	1.100	1.100	1.099	1.093	1.100	1.093	1.098
		d(CO)	1.387	1.398	1.412	1.431	1.554	1.377	1.252	1.323
		∠(HCH)	121.3	121.7	122.3	123.2	128.6	122.0	117.9	118.4
		ϕ	27.4	26.7	25.5	23.5	0.3	26.1	23.4	34.0
	$1\ ^3A''$	d(CH)	1.106	1.106	1.105	1.105	1.104	1.105	1.101	1.084
		d(CO)	1.350	1.356	1.362	1.369	1.378	1.355	1.251	1.307
		∠(HCH)	116.8	117.2	117.6	118.1	118.4	118.3	112.1	121.8
		ϕ	40.3	39.9	39.6	39.1	38.5	38.5	41.9	41.1
CH_2S	1^1A_2	d(CH)	1.096	1.096	1.096	1.096	1.097	1.096	1.082	1.077
		d(CS)	1.755	1.762	1.77	1.778	1.789	1.728	1.645	1.682
		∠(HCH)	120.9	121.1	121.3	121.4	121.7	121.2	119.0	120.7
	$1^3A''$	d(CH)	1.097	1.097	1.098	1.098	1.098	1.095	1.080	1.082
		d(CS)	1.727	1.732	1.736	1.741	1.747	1.711	1.638	1.683
		∠(HCH)	119.1	119.2	119.3	119.5	119.5	120.7	119.6	119.3
		ϕ	23.8	23.8	23.7	23.6	23.5	15.3	0.2	11.9
trans-$(CHO)_2$	1^1A_u	d(CC)	1.499	1.497	1.496	1.494	1.492	1.492	1.508	1.460
		d(CH)	1.105	1.105	1.104	1.104	1.104	1.106	1.094	1.115
		d(CO)	1.260	1.262	1.263	1.265	1.268	1.270	1.201	1.252
		∠(HCC)	115.0	115.2	115.3	115.5	115.6	114.8	112.7	114.0
		∠(OCC)	123.5	123.5	123.4	123.4	123.3	123.8	123.5	123.7
HC_2CHO	$1^1A''$	$d(C_1C_2)$	1.240	1.241	1.242	1.242	1.243	1.258	1.206	1.238
		$d(C_3H)$	1.094	1.094	1.093	1.092	1.092	1.096	1.083	1.091
		$d(C_3O)$	1.445	1.467	1.493	1.520	1.547	1.430	1.262	1.325
bond length	MSE		0.040	0.042	0.045	0.047	0.053	0.045	−0.009	
	MAE		0.044	0.046	0.048	0.051	0.057	0.048	0.030	
	RMSE		0.068	0.072	0.076	0.081	0.091	0.064	0.042	
	MAXE		0.283	0.299	0.313	0.326	0.339	0.208	0.160	
bond angle[e]	MSE		−0.004	−0.003	−0.002	0.000	0.007	0.001	−0.037	
	MAE		0.024	0.025	0.027	0.028	0.036	0.030	0.076	
	RMSE		0.035	0.035	0.036	0.037	0.056	0.038	0.125	
	MAXE		0.087	0.080	0.073	0.084	0.178	0.072	0.386	

[a] Statistical errors were separately calculated for bond lengths and bond angles. See Table 1 for other details. Bond lengths are in angstroms. [b] Bond angles and dihedral angles are in degrees. [c] Experimental references are summarized in ref 7. [d] Basis set defined in ref 7. [e] Errors in angles are in radians.

TABLE 5: Geometrical Parameters Optimized with aug-cc-pVTZ Basis[a,b]

			c_U							
molecule	state	parameter	1.30	1.35	1.40	1.45	1.51	CC2	CIS	exp[c]
Li_2[d]	$1^1\Sigma_u^+$	r_e	3.124	3.127	3.134	3.136	3.138	3.076	3.079	3.107
BH	$1^1\Pi$	r_e	1.197	1.198	1.198	1.198	1.198	1.210	1.203	1.219
BF	$1^1\Pi$	r_e	1.312	1.313	1.314	1.315	1.317	1.324	1.287	1.304
	$1^3\Pi$	r_e	1.317	1.317	1.317	1.317	1.317	1.329	1.301	1.308
	$1^3\Sigma^+$	r_e	1.213	1.213	1.213	1.213	1.214	1.230	1.203	1.215
N_2	$1^3\Pi_g$	r_e	1.220	1.221	1.221	1.222	1.223	1.256	1.177	1.213
	$1^1\Sigma_u^-$	r_e	1.271	1.272	1.272	1.273	1.273	1.311	1.234	1.276
	$1^1\Pi_g$	r_e	1.235	1.236	1.237	1.237	1.238	1.273	1.192	1.220
	$1^1\Delta_u$	r_e	1.267	1.267	1.268	1.268	1.269	1.299	1.230	1.268
CO	$1^1\Pi$	r_e	1.263	1.266	1.269	1.272	1.275	1.298	1.213	1.235
	$1^3\Pi$	r_e	1.208	1.209	1.209	1.210	1.211	1.236	1.177	1.206
Mg_2[d]	$1^1\Sigma_u^+$	r_e	3.065	3.065	3.065	3.064	3.063	3.146	2.797	3.082
SiO	$1^1\Pi$	r_e	1.718	1.723	1.729	1.735	1.743	1.758	1.582	1.620
	$1^3\Delta$	r_e	1.937	1.963	1.987	2.007	2.028	1.858	1.650	1.715
H_2O	2^1B_1	d(OH)	1.003	1.004	1.005	1.006	1.008	1.033	0.965	1.069
		∠(HOH)	105.0	105.0	104.9	104.8	104.7	102.1	109.3	101.6
SO_2	1^3B_1	d(SO)	1.519	1.522	1.526	1.530	1.534	1.564	1.445	1.494
		∠(OSO)	126.6	126.3	126.0	125.7	125.3	129.1	126.6	126.1
SiF_2	1^1B_1	d(SiF)	1.624	1.626	1.628	1.630	1.632	1.635	1.583	1.601
		∠(FSiF)	115.7	115.9	116.1	116.2	116.5	116.2	111.5	115.9
CCl_2	1^1B_1	d(CCl)	1.657	1.658	1.658	1.658	1.658	1.654	1.653	1.652
		∠(ClCCl)	133.2	133.0	133.0	133.0	133.0	132.0	132.8	131.4
CS_2	1^3A_2	d(CS)	1.642	1.643	1.645	1.646	1.647	1.654	1.595	1.640
		∠(SCS)	134.7	134.6	134.4	134.3	134.1	135.5	144.9	135.8
HCN	$1^1A''$	d(CH)	1.106	1.107	1.107	1.108	1.109	1.116	1.095	1.140
		d(CN)	1.292	1.292	1.292	1.292	1.292	1.324	1.284	1.297
		∠(HCN)	123.9	123.9	123.9	124.0	124.0	122.3	120.7	125.0
HCP	$1^1A''$	d(CP)	1.695	1.695	1.694	1.694	1.694	1.721	1.682	1.690
		∠(HCP)	130.1	130.2	130.6	130.7	130.7	128.0	132.0	128.0
C_3	$1^1\Pi_u$	d(CC)	1.297	1.297	1.298	1.298	1.298	1.326	1.285	1.305
C_2H_2	1^1A_u	d(CC)	1.369	1.370	1.371	1.371	1.372	1.384	1.352	1.375
		d(CH)	1.086	1.086	1.086	1.086	1.086	1.093	1.079	1.105
		∠(HCC)	121.6	121.5	121.4	121.3	121.2	121.8	124.7	121.4
CH_2O	$1^1A''$	d(CH)	1.085	1.085	1.084	1.084	1.083	1.088	1.086	1.098
		d(CO)	1.357	1.366	1.375	1.387	1.405	1.361	1.246	1.323
		∠(HCH)	120.1	120.5	120.8	121.5	122.3	121.6	117.9	118.4
		ϕ	28.8	28.4	28.0	27.1	25.7	25.7	21.8	34.0
	$1^3A''$	d(CH)	1.091	1.090	1.089	1.089	1.088	1.093	1.093	1.084
		d(CO)	1.329	1.334	1.340	1.346	1.353	1.341	1.245	1.307
		∠(HCH)	116.3	116.6	117.0	117.4	117.9	117.9	112.5	121.8
		ϕ	39.9	39.6	39.3	39.0	38.5	38.1	40.4	41.1
CH_2S	1^1A_2	d(CH)	1.078	1.078	1.078	1.078	1.079	1.083	1.086	1.077
		d(CS)	1.724	1.730	1.736	1.743	1.752	1.711	1.563	1.682
		∠(HCH)	120.5	120.6	120.5	120.7	120.9	121.1	118.7	120.7
	$1^3A''$	d(CH)	1.079	1.079	1.079	1.079	1.079	1.083	1.073	1.082
		d(CS)	1.699	1.703	1.707	1.712	1.717	1.694	1.624	1.683
		∠(HCH)	119.4	119.5	119.5	119.6	119.7	120.6	119.2	119.3
		ϕ	20.0	20.1	20.3	20.5	20.5	15.4	0.3	11.9
trans-$(CHO)_2$	1^1A_u	d(CC)	1.482	1.480	1.478	1.476	1.473	1.480	2.039	1.460
		d(CH)	1.088	1.088	1.088	1.087	1.087	1.095	1.087	1.115
		d(CO)	1.242	1.244	1.246	1.248	1.250	1.258	1.118	1.252
		∠(HCC)	114.2	114.4	114.6	114.7	114.9	114.5	101.9	114.0
		∠(OCC)	123.9	123.9	123.8	123.8	123.7	123.9	116.2	123.7
HC_2CHO	$1^1A''$	d(C_1C_2)	1.218	1.219	1.220	1.221	1.221	1.239	1.191	1.238
		d(C_3H)	1.079	1.079	1.078	1.077	1.076	1.085	1.077	1.091
		d(C_3O)	1.412	1.429	1.450	1.479	1.521	1.412	1.258	1.325
bond length	MSE		0.011	0.013	0.016	0.018	0.022	0.025	−0.026	
	MAE		0.025	0.027	0.029	0.031	0.035	0.032	0.037	
	RMSE		0.046	0.051	0.056	0.061	0.068	0.045	0.047	
	MAXE		0.222	0.248	0.272	0.292	0.313	0.143	0.159	
bond angle[e]	MSE		0.003	0.003	0.004	0.006	0.007	0.004	0.005	
	MAE		0.023	0.022	0.023	0.024	0.026	0.022	0.060	
	RMSE		0.035	0.034	0.034	0.034	0.035	0.031	0.081	
	MAXE		0.096	0.091	0.084	0.077	0.068	0.068	0.162	

[a] See Tables 1 and 4 for other details. Bond lengths are in angstroms. [b] Bond angles and dihedral angles are in degrees. [c] Experimental references are summarized in ref 7. [d] Basis set defined in ref 7. [e] Errors in angles are in radians.

theories is somewhat poorer for excited state problems than MP2 is for the ground state. Finally, relative to the nondegenerate second-order perturbation corrections, CIS(D), or its scaled opposite spin version, SOS-CIS(D), we expect that SOS-CIS(D_0) is substantially more reliable because of its correct treatment of quasi-degeneracies. As has been documented previously,[7,38] CIS(D) itself can be quite erratic for excited state geometries. Issues such as the incorrect pyramidalization angle for the $^1A''$ state of formaldehyde are largely corrected though CO bond length overestimation remains considerable.

TABLE 6: Geometrical Parameters Optimized with aug-cc-pVQZ Basis[a,b]

			c_U							
molecule	state	parameter	1.30	1.35	1.40	1.45	1.51	CC2	CIS	exp[c]
BH	$1^1\Pi$	r_e	1.204	1.205	1.206	1.206	1.206	1.209	1.203	1.219
BF	$1^1\Pi$	r_e	1.311	1.312	1.313	1.314	1.316	1.318	1.284	1.304
	$1^3\Pi$	r_e	1.316	1.316	1.316	1.316	1.316	1.323	1.299	1.308
	$1^3\Sigma^+$	r_e	1.211	1.211	1.211	1.212	1.212	1.224	1.200	1.215
N_2	$1^3\Pi_g$	r_e	1.220	1.221	1.222	1.223	1.223	1.251	1.176	1.213
	$1^1\Sigma_u^-$	r_e	1.273	1.273	1.274	1.274	1.275	1.307	1.233	1.276
	$1^1\Pi_g$	r_e	1.235	1.236	1.237	1.238	1.239	1.268	1.190	1.220
	$1^1\Delta_u$	r_e	1.268	1.268	1.269	1.270	1.270	1.295	1.228	1.268
CO	$1^1\Pi$	r_e	1.262	1.265	1.268	1.271	1.274	1.290	1.210	1.235
	$1^3\Pi$	r_e	1.207	1.208	1.209	1.210	1.211	1.230	1.175	1.206
SiO	$1^1\Pi$	r_e	1.700	1.706	1.711	1.718	1.725	1.747	1.574	1.620
	$1^3\Delta$	r_e	1.922	1.952	1.979	2.002	2.024	1.852	1.642	1.715
H_2O	$2\ ^1B_1$	d(OH)	0.998	0.999	1.000	1.001	1.002	1.021	0.962	1.069
		∠(HOH)	106.0	105.9	105.9	105.7	105.7	103.2	109.5	101.6
SO_2	$1\ ^3B_1$	d(SO)	1.507	1.510	1.513	1.517	1.521	1.554	1.436	1.494
		∠(OSO)	126.8	126.6	126.3	126.1	125.7	128.8	126.7	126.1
SiF_2	$1\ ^1B_1$	d(SiF)	1.609	1.611	1.612	1.614	1.616	1.628	1.575	1.601
		∠(FSiF)	116.3	116.5	116.7	116.8	117.1	115.9	111.5	115.9
CCl_2	$1\ ^1B_1$	d(CCl)	1.654	1.654	1.654	1.655	1.655	1.648	1.649	1.652
		∠(ClCCl)	132.9	132.9	132.9	132.9	132.9	132.0	133.0	131.4
CS_2	$1\ ^3A_2$	d(CS)	1.640	1.642	1.643	1.644	1.646	1.649	1.590	1.640
		∠(SCS)	134.6	134.4	134.3	134.2	134.0	135.7	146.0	135.8
HCN	$1\ ^1A''$	d(CH)	1.111	1.111	1.112	1.112	1.113	1.115	1.095	1.140
		d(CN)	1.293	1.293	1.293	1.294	1.294	1.321	1.282	1.297
		∠(HCN)	123.7	123.7	123.8	123.8	123.8	122.3	120.8	125.0
HCP	$1\ ^1A''$	d(CP)	1.692	1.691	1.691	1.690	1.690	1.716	1.676	1.690
		∠(HCP)	129.6	129.8	130.1	130.2	130.2	128.4	132.8	128.0
C_3	$1\ ^1\Pi_u$	d(CC)	1.299	1.299	1.299	1.300	1.300	1.322	1.284	1.305
C_2H_2	$1\ ^1A_u$	d(CC)	1.369	1.370	1.371	1.371	1.372	1.381	1.351	1.375
		d(CH)	1.089	1.089	1.089	1.090	1.090	1.092	1.079	1.105
		∠(HCC)	121.9	121.9	121.7	121.6	121.5	122.0	124.8	121.4
CH_2O	$1\ ^1A''$	d(CH)	1.087	1.087	1.086	1.086	1.085	1.087	1.086	1.098
		d(CO)	1.354	1.362	1.371	1.382	1.399	1.355	1.244	1.323
		∠(HCH)	120.1	120.5	121.0	121.4	122.2	121.6	117.8	118.4
		ϕ	28.7	28.4	27.9	27.2	25.8	25.7	21.8	34.0
	$1\ ^3A''$	d(CH)	1.092	1.092	1.091	1.090	1.090	1.092	1.094	1.084
		d(CO)	1.326	1.331	1.337	1.342	1.350	1.336	1.243	1.307
		∠(HCH)	116.3	116.6	117.0	117.4	117.8	118.0	112.3	121.8
		ϕ	39.9	39.6	39.3	39.0	38.5	38.1	40.6	41.1
CH_2S	$1\ ^1A_2$	d(CH)	1.081	1.081	1.081	1.081	1.082	1.083	1.086	1.077
		d(CS)	1.717	1.723	1.729	1.736	1.744	1.706	1.560	1.682
		∠(HCH)	120.4	120.6	120.7	120.9	121.1	121.2	118.5	120.7
	$1\ ^3A''$	d(CH)	1.081	1.081	1.082	1.082	1.082	1.082	1.072	1.082
		d(CS)	1.693	1.697	1.701	1.706	1.711	1.689	1.620	1.683
		∠(HCH)	119.6	119.7	119.7	119.8	120.0	120.5	119.1	119.3
		ϕ	18.6	18.6	18.7	18.8	18.3	15.0	1.9	11.9
trans-$(CHO)_2$	$1\ ^1A_u$	d(CC)	1.483	1.480	1.478	1.476	1.473	1.479	2.042	1.460
		d(CH)	1.092	1.092	1.092	1.091	1.091	1.095	1.087	1.115
		d(CO)	1.241	1.243	1.245	1.247	1.249	1.254	1.116	1.252
		∠(HCC)	114.5	114.6	114.8	115.0	115.2	114.5	101.8	114.0
		∠(OCC)	123.8	123.7	123.7	123.6	123.6	123.9	116.2	123.7
HC_2CHO	$1\ ^1A''$	$d(C_1C_2)$	1.217	1.218	1.219	1.220	1.220	1.238	1.191	1.238
		$d(C_3H)$	1.081	1.081	1.080	1.079	1.078	1.085	1.077	1.091
		$d(C_3O)$	1.408	1.425	1.444	1.473	1.514	1.406	1.256	1.325
bond length	MSE		0.010	0.012	0.015	0.018	0.021	0.021	−0.033	
	MAE		0.022	0.024	0.026	0.029	0.032	0.028	0.036	
	RMSE		0.043	0.049	0.054	0.060	0.067	0.041	0.043	
	MAXE		0.207	0.237	0.264	0.287	0.309	0.137	0.107	
bond angle[d]	MSE		0.004	0.005	0.007	0.008	0.010	0.006	0.007	
	MAE		0.025	0.025	0.026	0.026	0.028	0.023	0.064	
	RMSE		0.037	0.036	0.036	0.036	0.037	0.031	0.086	
	MAXE		0.096	0.091	0.084	0.077	0.072	0.066	0.178	

[a] See Tables 1 and 4 for other details. Bond lengths are in angstroms. [b] Bond angles and dihedral angles are in degrees. [c] Experimental references are summarized in ref 7. [d] Errors in angles are in radians.

4. Application

The SOS-CIS(D_0) theory with this optimal scaling parameter, $c_U = 1.40$, is applied to characterizing electronic transitions in 9-methyl-9,10-dihydro-9-silaphenanthrene. It was reported that this molecule exhibits a peculiarly large Stokes shift together with a broad fluorescence feature (∼300−400 nm) even at low temperature.[24] As the Stokes shift of the emission can be estimated in conjunction with the excited state geometry optimization, the molecule will be an interesting target for demonstrating the applicability of our new theory.

Figure 2 shows the potential energy surfaces of this molecule on its electronic ground (S_0) and first two excited states (S_1 and

TABLE 7: Adiabatic Excitation Energies (in eV) for $\pi \rightarrow \pi^*$ and n $\rightarrow \pi^*$ Transitions of Selected Organic Molecules with Different Qualities of Basis Sets

				basis		
	molecule[a]	no.	sym	aug-cc-pVTZ	6-31+G(d)	exp[b]
$\pi \rightarrow \pi^*$	hexatriene	1	^1B_u	4.76	4.84	4.93
	benzene	2	$^1B_{1u}$	6.03	6.16	6.03
		3	$^1B_{2u}$	4.88	4.84	4.72
		4	$^1E_{1u}$	7.23	7.30	6.87
	phenol	5	$^1A'$	4.61	4.59	4.51
	benzaldehyde	6	$^1A'$	5.23	5.24	5.12
	styrene	7	$^1A'$	5.04	5.14	4.88
		8	$^1A'$	4.55	4.56	4.31
	octatetraene	9	^1B_u	4.43	4.55	4.41
	naphthalene	10	$^1B_{2u}$	4.61	4.72	4.45
		11	$^1B_{3u}$	4.19	4.15	3.96
	azulene	12	$^1B_1$	1.69	1.65	1.77
	indole	13	$^1A'$ (L_a)	5.03[c]	5.06[c]	4.54
		14	$^1A'$ (L_b)	4.53	4.51	4.37
	p-diethynylbenzene	15	$^1B_{2u}$	4.54	4.49	4.25
	biphenylene	16	$^1B_{3u}$	3.73	3.72	3.55
	trans-stilbene	17	^1B_u	4.03	4.21	4.00
	anthracene	18	$^1B_{2u}$	3.61	3.69	3.43
	pyrene	19	$^1B_{2u}$	3.94	3.61	3.81
		20	$^1B_{3u}$	3.54	3.52	3.44
n $\rightarrow \pi^*$	acetone	21	$^1A_2$	3.39	3.19	3.76
	thioacetone	22	$^1A_2$	2.09	2.00	2.33
		23	$^3A_2$	1.98	1.86	2.14
	acrolein	24	$^1A''$	3.13	2.96	3.21
		25	$^3A''$	2.95	2.78	3.01
	2-cyclopenten-1-one	26	$^1A''$	3.25	3.09	3.36
		27	$^3A''$	3.16	2.95	3.22
	s-tetrazine	28	$^1B_{1u}$	2.35	2.46	2.25
	benzaldehyde	29	$^1A''$	3.14	2.99	3.34
		30	$^3A''$	3.01	2.83	3.12
	DMABN	31	$^1A_2$	4.21	4.22	3.95
	trans-azobenzene	32	$^1A_2$	2.33	2.46	2.60
MSE				0.05	0.02	
MAE				0.17	0.23	
RMSE				0.20	0.26	
MAXE				0.49	0.57	

[a] The geometry optimizations and the harmonic zero-point energy calculations were performed at SOS-MP2/6-31G(d) and SOS-CIS(D_0)/6-31+G(d) levels of theory for ground and excited state calculations, respectively. [b] Experimental data from ref 15. [c] Numerical Hessian on S_2 surface could not be obtained due to the surface crossing near the minimum, and transition energies without zero-point energy corrections were used in this case. See section 4 for the detailed explanation of the surface crossing issue.

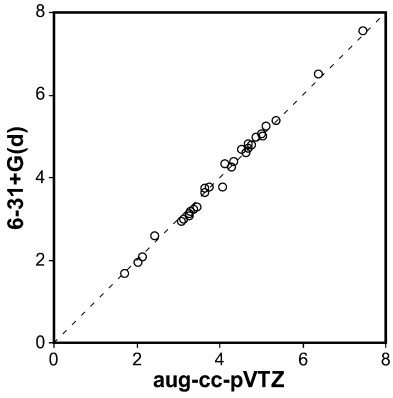

Figure 1. Comparison of vertical transition energies of the organic molecules in Table 7 estimated with basis sets of different qualities. Units are in electronvolts.

S_2). The electronic energies were obtained as functions of the interatomic distance between the methylene carbon and the silicon atom. (See the inset in Figure 2 for the location of this constrained bond.) All other bond lengths and angles were varied through the use of a constrained optimization algorithm.[39] The figure shows the excited state energies at the optimized ground state geometries and also the ground state energies at the optimized excited state (S_1) geometries with dotted lines. The two gaps between each pair of solid and dashed lines correspond to photon energies of the vertical absorption and emission, as marked with two arrows in the figure. Of course, the gaps from each of the energy minima will closely follow the most probable absorption/emission wavelengths or the spectral peak centers in the experiment. If we assume that both the absorption and the emission correspond to $S_0 \leftrightarrow S_1$ transition as implied in the experimental study,[24] the estimated peak positions from our calculations are 255 and 362 nm, respectively. These results are in good accord with the experimental values of 269 and 362 nm. Even though care must be taken in comparing these numbers directly, as the experiment was conducted in methylcyclohexane solution and the calculations were performed in the gas phase, this agreement is a quite encouraging observation.

In addition, because S_1 and S_2 are so close in energy, with ~0.1 eV gap for a wide range of values of the C−Si bond length, the two absorptions will not be separately resolved with the broad spectrum obtained from experiment.[24] In fact, at the ground state equilibrium geometry, the oscillator strength of $S_0 \rightarrow S_2$ transition is much larger than that of $S_0 \rightarrow S_1$ transition (0.017 versus 0.001), and therefore, presuming vibronic mixing[40]

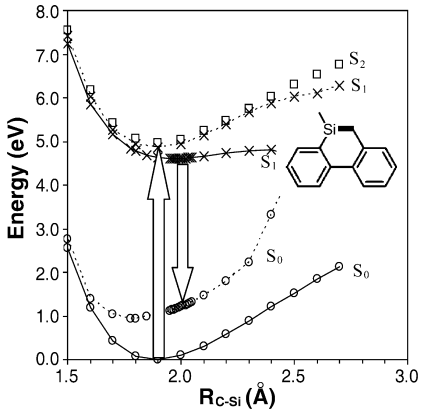

Figure 2. Potential energy surfaces of the electronic ground state (circles) and the first excited state (crosses) of 9-methyl-9,10-dihydro-9-silaphenanthrene. The energies are generated through geometry optimizations on each surface with the single constrained C−Si bond length. The constrained bond is shown with a thick line in the chemical structure. The lower dotted curve represents the electronic ground state energies at optimized excited state geometries, while the upper dotted one shows the excited state energies at ground state geometries. The arrows depict the energies of the most dominant absorption and emission. Squares represent the energies of the second excited state at the ground state geometries. The 6-31G** basis set was used for all computation together with the VDZ auxiliary basis set (ref 31). The adopted tolerance on the maximum Cartesian gradient component was 10^{-4} hartree/bohr.

is small, it is likely that the measured spectrum actually corresponds to the $S_0 \rightarrow S_2$ transition. (In Figure 2 of ref 24, a small shoulder peak can be seen on the red side of the main absorption peak. This may well be explained with our computational result, even though more experimental data will be needed to confirm this suggestion.) With this reasoning, our prediction of the absorption peak position is actually 249 nm, still in good agreement with the experimental number (269 nm). Even with this dominant $S_0 \rightarrow S_2$ transition, the emission will normally commence from S_1 and our prediction of the emission peak position in the above is not affected by this consideration. Of course, the major involvement of these two different states in the absorption and emission contributes to the unusually large Stoke shift observed in the molecule.

Indeed, the fast nonradiative transition from S_2 to S_1 can also be explained when one inspects the detailed nature of the two surfaces. As noted above, one interesting aspect of this molecule is the fact that it possesses a second singlet excited state (S_2) very close to S_1. To obtain the relative locations of the two lowest excited surfaces, another set of constrained geometry optimizations were performed starting from the equilibrium geometries on the S_1 surface, but by following the S_2 surface gradient. In this case, as the energy is lowered by the geometry search, there is always a possibility of encountering the seam of the conical intersection between S_1 and S_2. At any given C−Si constrained distance, there will be three different cases for the relative locations of S_1 and S_2 as schematically illustrated in Figure 3: (a) where the two surfaces do not cross during the optimization, (b) where the two surfaces cross far from the equilibrium geometry, and (c) where the two surfaces cross near the equilibrium of S_2 surface. Indeed, when any two states are exactly degenerate, the two corresponding eigenvectors may freely mix with each other, and the gradient becomes ill-defined. Case c above will be seriously affected by this, and the constrained optimization will not converge in practice on the desired surface unless the convergence criterion of the optimization is loosely defined.

Case (b) could be similarly affected near the seam of crossing, but because of the finite step sizes in geometry optimization, the optimization process may well skip this ill-defined region. Therefore the problem can be avoided as long as the state index switching after passing the degenerate point is detected. In other words, as long as the lower excited state is followed instead of the higher state after this crossing, the optimization will readily converge to the minimum point on the desired surface. To detect such crossings, we have utilized the approximate one-particle unrelaxed density matrix of the S_2 state[3,4,23]

$$P_{\mu\nu} = \sum_{i}^{\mathrm{occ}} C_{\mu i} C_{\nu i} - \sum_{a}^{\mathrm{virt}} \sum_{ij}^{\mathrm{occ}} b_i^a b_j^a C_{\mu i} C_{\nu j} + \sum_{i}^{\mathrm{occ}} \sum_{ab}^{\mathrm{virt}} b_i^a b_i^b C_{\mu a} C_{\nu b} \quad (9)$$

with $C_{\mu i}$ and $C_{\mu a}$ representing the molecular orbital coefficients of occupied ("occ") and virtual ("virt") orbitals, respectively. Of course, b_i^a represents the elements of the single excitation amplitude vector **b**, defined with eq 1. The approximation adopted in this equation compared to the full density matrix[23] is the omission of some terms related to electron-correlation and orbital relaxation effects. The purpose of using this approximation is simply to eliminate the computational cost associated with this state following scheme. Specifically, at each step of geometry optimization, we have compared **P** matrices of all computed excited states against the **P** matrix of the desired state at the previous optimization step, and followed the maximally overlapping one.

Figure 4 presents the relative locations of the two lowest excited states thus obtained. Because of the surface crossing, it is somewhat ambiguous to designate them as S_1 and S_2. We will adopt the conventional approach of assigning the surface with lower energy at the ground state equilibrium geometry as S_1. From Figure 4, it is interesting to see that the S_2 surface at its equilibrium (solid curve with squares at C−Si distance of ~1.9 Å) actually has lower energy than the S_1 surface (dotted curve with crosses). However, at the same C−Si distance, the S_1-optimized surface (solid curve with crosses) is still slightly lower than this optimized S_2 surface. From this, one can infer that any molecule oscillating on S_2 surface under solvent fluctuations will speedily meet the surface intersection with S_1 and experience a fast internal conversion to S_1. Thus, all emission will effectively commence from this state. One may wonder whether the resulting emission will be very weak due to the small oscillator strength mentioned above (0.001 at S_0 equilibrium). Quite understandably from the large Stokes shift, the molecule is highly distorted at S_1 equilibrium compared to the S_0 structure (See Figure 5 and Table 8 for the detailed depictions of the geometries), and the oscillator strength of the emission at S_1 equilibrium is as large as 0.200. This is consistent with the relatively high quantum yield (28%) for emission from this molecule at 77 K.[24] Also from Figure 2, one can predict that an S_0-S_1 conical intersection will eventually take place at large C−Si separation. As a single reference method, SOS-CIS(D_0) is not adequate for predicting this crossing. However, from the small curvature of the S_1 surface, we should expect that it will cross S_0 even with a relatively small amount of vibrational energy on S_1. Accordingly, nonradiative deactivation from S_1 will be promoted significantly even at moderate temperature. In fact, the experimental quantum yield for emission was found to be only 3% at room temperature.[24]

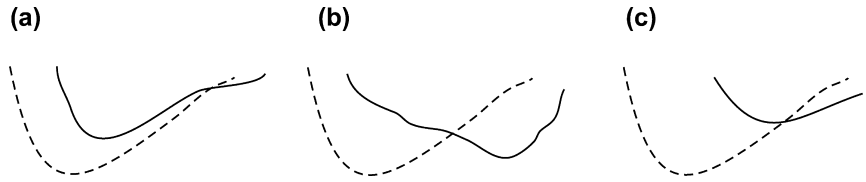

Figure 3. Schematic illustration of three different situations in performing constrained geometry optimizations of a polyatomic molecule on S_2 surface (solid lines) starting from the equilibrium geometries on S_1 surface (dashed lines). (a) The S_1 equilibrium geometry is a good initial guess and the search readily converges. (b) The search from the S_1 geometry passes through the surface intersection. In this case, the search can still converge if the state indices are properly switched after passing the intersection. (c) The S_2 minimum is near the seam of the intersection, and attaining convergence with a small tolerance is practically very difficult. In all cases, note that the horizontal axis represents a collective coordinate, which is orthogonal to the constrained bond.

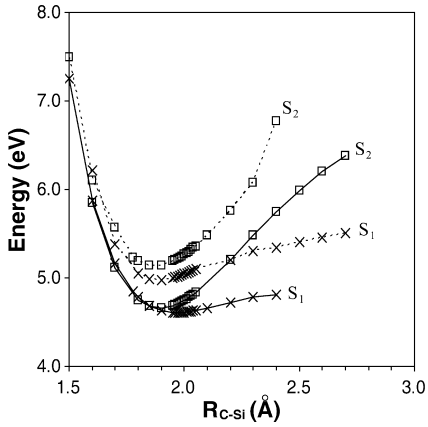

Figure 4. Potential energy surfaces of S_1 (crosses) and S_2 (squares) electronic states of 9-methyl-9,10-dihydro-9-silaphenanthrene. The energies are generated through geometry optimizations on each surface with the single constrained C−Si bond length. The lower dotted curve represents the energies of the S_1 state at S_2-optimized geometries, while the upper dotted curve represents the S_2 energies at S_1-optimized geometries. The adopted tolerance on the maximum Cartesian gradient component was 10^{-4} hartree/bohr except at 2.2 Å on S_2 surface, where 10^{-3} hartree/bohr tolerance was used instead. At 2.1 Å, optimization on a S_2 surface failed even with this loose tolerance. The 6-31G** basis set was used for all computation together with the VDZ auxiliary basis set.

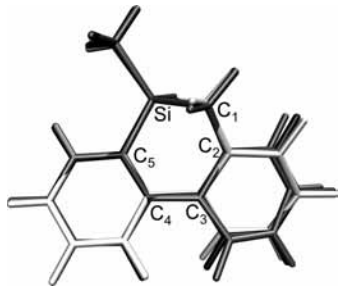

Figure 5. Optimized geometries of 9-methyl-9,10-dihydro-9-silaphenanthrene on S_0 (light gray), S_1 (medium gray), and S_2 (dark gray) electronic potential energy surfaces. One can see that the most notable difference is the relative twisting between the two phenyl rings. See Table 8 for detailed descriptions of geometric parameters. The S_1 and S_2 geometries are optimally aligned to S_0 conformation according to ref 65.

The broad emission feature observed from experiment can also be understood from the shape of the excited state surface: because the S_1 surface is very flat near the minimum, the excited molecule will sample a large range of C−Si distances. The vertical downward transitions from this wide range of excited geometries will result in emissions of photons with widely varying wavelength, because the ground state surface is not nearly as flat as the excited state surface. This is in qualitative agreement with semiempirical molecular orbital calculations on the unsubstituted 9,10-dihydrophenanthrene molecule.[24]

TABLE 8: Selected Geometric Parameters of Optimized Structures of 9-Methyl-9,10-dihydro-9-silaphenanthrene on the Three Electronic Potential Energy Surfaces[a]

	geometric parameter	S_0	S_1	S_2
bond length (Å)	r_{Si-C_1}	1.90	1.97	1.90
	$r_{C_1-C_2}$	1.52	1.46	1.49
	$r_{C_2-C_3}$	1.42	1.48	1.46
	$r_{C_3-C_4}$	1.49	1.41	1.42
	$r_{C_4-C_5}$	1.42	1.46	1.44
	r_{C_5-Si}	1.88	1.83	1.86
dihedral angle (deg)	$\phi_{C_2-C_3-C_4-C_5}$	34.8	7.2	23.4

[a] See Figure 5 for atomic designations.

Finally, we comment that higher excited states of the molecule will also have an active role in the photochemistry of this interesting molecule. In fact, the third excited state, S_3, is well separated from S_2 with a gap of ~0.5 eV at the ground state geometry with quite large oscillator strength (~0.4) for the associated $S_0 \rightarrow S_3$ transition at 227 nm. The unassigned large absorption peak reported experimentally in the short wavelength region (<230 nm) is well explained with our computational results for S_3. Even though this state is well separated from S_2 at the optimized ground state geometries, the gap decreases significantly at S_2-optimized geometries, and especially at short C−Si distances. Thus, molecules that are excited to S_3 will be efficiently funneled into S_2 and then ultimately down to S_1. Further calculations that trace the relaxation dynamics down to the ground state would be necessary to account for the experimental observation of photoinduced products including 9-silaphenanthrene upon photolysis with 266 nm light.

5. Conclusions

In summary, we have shown that a scaled opposite spin approach for the quasi-degenerate second-order perturbative correction to single excitation configuration interaction (SOS-CIS(D_0)) can be a reliable approach for predicting molecular excitation energies and excited state geometries. On the basis of a range of test calculations, we recommend choosing the excited state scaling parameter as $c_U = 1.4$, to accompany the ground state scaling parameter, $c_T = 1.3$, which is transferred from the SOS-MP2 method. When the SOS-CIS(D_0) method was applied to electronic transitions of 9-methyl-9,10-dihydro-9-silaphenanthrene, various experimental observations could be explained with our theory. It is stressed that the capability of SOS-CIS(D_0) to properly describe quasi-degenerate excited states is crucial to achieving this reliability. With the previously shown quartic-scaling efficiency of the theory,[23] SOS-CIS(D_0) becomes useful for practical applications to many chemical systems. Relative to other methods, SOS-CIS(D_0) yields results whose accuracy approaches that of the quite well-established CC2 method, which has computational costs that scale with the

fifth power of molecular size. We note that spin-component scaling ideas have also been very recently applied to the CC2 model,[41] and a similar quartic-scaling SOS-CC2 theory that retains only opposite spin correlations could be developed. In fact, all these developmental efforts can be viewed in the same context as the continuing efforts to develop mixed quantum mechanics and molecular mechanics (QM/MM)[42−47] methods and the more generalized ONIOM[48,49] methods, and other related energy partitioning schemes.[50,51] All these endeavors are focused on developing efficient and reliable methods that can be applied to large and complex systems, and we may well benefit in the future by combining these approaches in a hybridized manner.

To this stage, time-dependent density functional theory (TDDFT) and the configuration interaction singles (CIS) method have been the only practically applicable excited state approaches with gradients for molecules too large to be treated by CC2 or still more expensive excited state coupled cluster methods. Because both of these methods have their own limitations such as TDDFT seriously underestimating long-range charge transfer transition energies,[52−60] or CIS commonly yielding errors of an electronvolt or more, our SOS-CIS(D_0) method may be useful for a range of applications to interesting molecules. Indeed, excited state dynamics is crucial for understanding many photophysical processes, and since SOS-CIS(D_0) is capable of properly describing interactions between various electronic excited states, it will open various possibilities for theoretically studying such processes.

In concluding, it must be reiterated that SOS-CIS(D_0) is a one-parameter semiempirical method, and therefore the validity (or transferability) of the scaling parameter that we have determined in this work will still need to be verified for other molecular systems. Also, it is expected that excited states with characteristics that are very different from the ones we trained on may not be described with an equal level of success. One obvious example is the case of core electron excitations with large ω noted by Besley and co-workers, where the approximation of $\mathbf{D}^{(0)} - \omega \approx \mathbf{D}^{(0)}$ (ref 10) for eq 2 inevitably fails.[61] Nevertheless, we are reasonably encouraged by the results reported here regarding various valence and Rydberg type of transitions, which suggests that a range of parameter values can work quite well (suggesting reasonable transferability of our chosen value). An additional limitation is that, as a single-excitation based method, SOS-CIS(D_0) is not capable of describing states with significant bielectronic character. There is some encouraging progress toward simple methods that can describe some states of this type.[62−64] Despite these limitations, the advantages of SOS-CIS(D_0) (reasonably good accuracy for one-electron excited states in a low-scaling method without self-interaction errors) make it a useful new alternative for exploring excited state potential energy surfaces of molecules too large to treat by coupled cluster or CC2 methods.

Acknowledgment. This work was supported by the Director, Office of Energy Research, Office of Basic Energy Sciences, Chemical Sciences Division of the U.S. Department of Energy under Contract No. DE-AC0376SF00098. We are grateful for a grant of supercomputer time from NERSC, and also from Korea Institute of Science and Technology Information (KISTI) under Grant No. KSC-2009-S01-0008. D.C. acknowledges a financial support from Fulbright Fellowship. M.H.G. is a part-owner of Q-Chem Inc.

References and Notes

(1) Runge, E.; Gross, E. K. U. *Phys. Rev. Lett.* **1984**, *52*, 997.
(2) Furche, F.; Ahlrichs, R. *J. Chem. Phys.* **2002**, *117*, 7433.
(3) Foresman, J. B.; Head-Gordon, M.; Pople, J. A.; Frisch, M. J. *J. Phys. Chem.* **1992**, *96*, 135.
(4) Maurice, D.; Head-Gordon, M. *Mol. Phys.* **1999**, *96*, 1533.
(5) Bartlett, R. J. *Modern Electronic Structure Theory*; World Scientific: Singapore, 1995.
(6) Sekino, H.; Bartlett, R. J. *Int. J. Quantum Chem. Symp.* **1984**, *18*, 225.
(7) Köhn, A.; Hättig, C. *J. Chem. Phys.* **2003**, *119*, 5021.
(8) Christiansen, O.; Koch, H.; Jørgensen, P. *Chem. Phys. Lett.* **1995**, *243*, 409.
(9) Head-Gordon, M.; Rico, R. J.; Oumi, M.; Lee, T. J. *Chem. Phys. Lett.* **1994**, *219*, 21.
(10) Head-Gordon, M.; Oumi, M.; Maurice, D. *Mol. Phys.* **1999**, *96*, 593.
(11) Jung, Y.; Lochan, R. C.; Dutoi, A. D.; Head-Gordon, M. *J. Chem. Phys.* **2004**, *121*, 9793.
(12) Lochan, R. C.; Jung, Y.; Head-Gordon, M. *J. Phys. Chem. A* **2005**, *109*, 7598.
(13) Lochan, R. C.; Shao, Y. H.; Head-Gordon, M. *J. Chem. Theory Comput.* **2007**, *3*, 988.
(14) Grimme, S. *J. Chem. Phys.* **2003**, *118*, 9095.
(15) Grimme, S.; Izgorodina, E. I. *Chem. Phys.* **2004**, *305*, 223.
(16) Szabados, A. *J. Chem. Phys.* **2006**, *125*, 214105.
(17) Almlöf, J. *Chem. Phys. Lett.* **1991**, *181*, 319.
(18) Häser, M.; Almlöf, J. *J. Chem. Phys.* **1992**, *96*, 489.
(19) Izmaylov, A. F.; Scuseria, G. E. *Phys. Chem. Chem. Phys.* **2008**, *10*, 3421.
(20) Kats, D.; Usvyat, D.; Schütz, M. *Phys. Chem. Chem. Phys.* **2008**, *10*, 3430.
(21) Rhee, Y. M.; Head-Gordon, M. *J. Phys. Chem. A* **2007**, *111*, 5314.
(22) Casanova, D.; Rhee, Y. M.; Head-Gordon, M. *J. Chem. Phys.* **2008**, *128*, 164106.
(23) Rhee, Y. M.; Casanova, D.; Head-Gordon, M. *J. Chem. Theory Comput.* **2009**, *5*, 1224.
(24) Hiratsuka, H.; Horiuchi, H.; Furukawa, Y.; Watanabe, H.; Ishihara, A.; Okutsu, T.; Tobita, S.; Yoshinaga, T.; Shinohara, A.; Tokitoh, N.; Oba, M.; Nishiyama, K. *J. Phys. Chem. A* **2006**, *110*, 3868.
(25) DiStasio Jr, R. A.; Steele, R. P.; Rhee, Y. M.; Shao, Y.; Head-Gordon, M. *J. Comput. Chem.* **2007**, *28*, 839.
(26) Feyereisen, M.; Fitzgerald, G.; Komornicki, A. *Chem. Phys. Lett.* **1993**, *208*, 359.
(27) Hättig, C.; Hald, K. *Phys. Chem. Chem. Phys.* **2002**, *4*, 2111.
(28) Hättig, C.; Weigend, F. *J. Chem. Phys.* **2000**, *113*, 5154.
(29) Vahtras, O.; Almlöf, J.; Feyereisen, M. W. *Chem. Phys. Lett.* **1993**, *213*, 514.
(30) Weigend, F.; Häser, M. *Theo. Chem. Acc.* **1997**, *97*, 331.
(31) Weigend, F.; Häser, M.; Patzelt, H.; Ahlrichs, R. *Chem. Phys. Lett.* **1998**, *294*, 143.
(32) Werner, H.-J.; Manby, F. R.; Knowles, P. J. *J. Chem. Phys.* **2003**, *118*, 8149.
(33) Pulay, P. *Mol. Phys.* **1969**, *17*, 197.
(34) Handy, N. C.; Amos, R. D.; Gaw, J. F.; Rice, J. E.; Simandrias, E. D. *Chem. Phys. Lett.* **1985**, *120*, 151.
(35) Szabo, A.; Ostlund, N. S. *Modern Quantum Chemistry: Introduction to Advanced Electronic Structure Theory*; McGraw-Hill: New York, 1989.
(36) Handy, N. C.; Schaefer, H. F. *J. Chem. Phys.* **1984**, *81*, 503.
(37) Shao, Y.; Molnar, L. F.; Jung, Y.; Kussmann, J.; Ochsenfeld, C.; Brown, S. T.; Gilbert, A. T. B.; Slipchenko, L. V.; Levchenko, S. V.; O'Neill, D. P.; Distasio, R. A.; Lochan, R. C.; Wang, T.; Beran, G. J. O.; Besley, N. A.; Herbert, J. M.; Lin, C. Y.; van Voorhis, T.; Chien, S. H.; Sodt, A.; Steele, R. P.; Rassolov, V. A.; Maslen, P. E.; Korambath, P. P.; Adamson, R. D.; Austin, B.; Baker, J.; Byrd, E. F. C.; Dachsel, H.; Doerksen, R. J.; Dreuw, A.; Dunietz, B. D.; Dutoi, A. D.; Furlani, T. R.; Gwaltney, S. R.; Heyden, A.; Hirata, S.; Hsu, C.-P.; Kedziora, G.; Khalliulin, R. Z.; Klunzinger, P.; Lee, A. M.; Lee, M. S.; Liang, W.; Lotan, I.; Nair, N.; Peters, B.; Proynov, E. I.; Pieniazek, P. A.; Rhee, Y. M.; Ritchie, J.; Rosta, E.; Sherrill, C. D.; Simmonett, A. C.; Subotnik, J. E.; Woodcock, H. L., III; Zhang, W.; Bell, A. T.; Chakraborty, A. K.; Chipman, D. M.; Keil, F. J.; Warshel, A.; Hehre, W. J.; Schaefer III, H. F.; Kong, J.; Krylov, A. I.; Gill, P. M. W.; Head-Gordon, M. *Phys. Chem. Chem. Phys.* **2006**, *8*, 3172.
(38) Stanton, J. F.; Gauss, J.; Ishikawa, N.; Head-Gordon, M. *J. Chem. Phys.* **1995**, *103*, 4160.
(39) Baker, J. *J. Comput. Chem.* **1986**, *7*, 385.
(40) Lathrop, E. J. P.; Friesner, R. A. *J. Phys. Chem.* **1994**, *98*, 3050.
(41) Hellweg, A.; Grun, S. A.; Hättig, C. *Phys. Chem. Chem. Phys.* **2008**, *10*, 4119.
(42) Warshel, A.; Levitt, M. *J. Mol. Biol.* **1976**, *103*, 227.
(43) Field, M. J.; Bash, P. A.; Karplus, M. *J. Comput. Chem.* **1990**, *11*, 700.
(44) Singh, U. C.; Kollman, P. A. *J. Comput. Chem.* **1986**, *7*, 718.
(45) Hayashi, S.; Ohmine, I. *J. Phys. Chem. B* **2000**, *104*, 10678.
(46) Philipp, D. M.; Friesner, R. A. *J. Comput. Chem.* **1999**, *20*, 1468.

(47) Zhang, Y.; Lin, H.; Truhlar, D. G. *J. Chem. Theory Comput.* **2007**, *3*, 1378.
(48) Kerdcharoen, T.; Morokuma, K. *Chem. Phys. Lett.* **2002**, *355*, 257.
(49) Svensson, M.; Humbel, S.; Froese, R. D. J.; Matsubara, T.; Sieber, S.; Morokuma, K. *J. Phys. Chem.* **1996**, *100*, 19357.
(50) Wesolowski, T. A.; Warshel, A. *J. Phys. Chem.* **1993**, *97*, 8050.
(51) Beran, G. J. O. *J. Chem. Phys.* **2009**, *130*, 164115.
(52) Casida, M. E.; Gutierrez, F.; Guan, J.; Gadea, F.-X.; Salahub, D.; Daudey, J.-P. *J. Chem. Phys.* **2000**, *113*, 7062.
(53) Dreuw, A.; Head-Gordon, M. *J. Am. Chem. Soc.* **2004**, *126*, 4007.
(54) Neugebauer, J.; Gritsenko, O.; Baerends, E. J. *J. Chem. Phys.* **2006**, *124*, 214101.
(55) Hieringer, W.; Görling, A. G. *Chem. Phys. Lett.* **2006**, *426*, 234.
(56) Hieringer, W.; Görling, A. G. *Chem. Phys. Lett.* **2006**, *419*, 557.
(57) Dreuw, A.; Head-Gordon, M. *Chem. Phys. Lett.* **2006**, *426*, 231.
(58) Izmaylov, A. F.; Scuseria, G. E. *J. Chem. Phys.* **2008**, *129*, 034101.
(59) Giesbertz, K. J. H.; Baerends, E. J. *Chem. Phys. Lett.* **2008**, *461*, 338.
(60) Gritsenko, O.; van Gisbergen, S. J. A.; Görling, A.; Baerends, E. J. *J. Chem. Phys.* **2000**, *113*, 8478.
(61) Asmuruf, F. A.; Besley, N. A. *Chem. Phys. Lett.* **2008**, *463*, 267.
(62) Casanova, D.; Slipchenko, L. V.; Krylov, A. I.; Head-Gordon, M. *J. Chem. Phys.* **2009**, *130*, 044103.
(63) Casanova, D.; Head-Gordon, M. *J. Chem. Phys.* **2008**, *129*, 064104.
(64) Krylov, A. I. *Chem. Phys. Lett.* **2001**, *350*, 522.
(65) Rhee, Y. M. *J. Chem. Phys.* **2000**, *113*, 6021.

JP903659U